

## Degradation of Phenol in the System TiO<sub>2</sub> Nanoparticles and N-Containing Compound

<sup>1</sup>Sevinj Hajiyeva, <sup>1</sup>Elmina Gadirova, <sup>2</sup>Afsun Sujayev\*, <sup>3</sup>Nedim Ozdemir

<sup>1</sup>Baku State University, Ecological Chemistry Department, 1148, Baku, Azerbaijan

<sup>2</sup>Laboratory of Fine Organic chemistry, Institute of Chemistry of Additives, 1029, Baku, Azerbaijan

<sup>3</sup>Mugla Sitki Kocman University, 48000, Mugla, Turkey

sucayevafsun@gmail.com; s.afsun@mail.ru

(Received on 26<sup>th</sup> November 2021, accepted in revised form 22<sup>nd</sup> April 2022)

**Summary:** The purpose this research was to study the decomposition of phenol in water under the influence of UV radiation in the presence of nanoparticles TiO<sub>2</sub> and methyl-3-amicronate.

The photochemical decomposition of phenol in the presence of UV in a system of TiO<sub>2</sub>+N containing substances was carried out. The TiO<sub>2</sub> nanoparticles used in the reaction had a size from 10 to 30 nm and belonged to the rutile phase. Nano-TiO<sub>2</sub> was studied by X-ray diffraction, TEM and SEM methods. All the XRD peaks were well-defined and corresponded to rutile phase TiO<sub>2</sub>. From the line broadening of the (101) diffraction peak by Scherrer's method, the average crystal size TiO<sub>2</sub> is about 10.3. The specific surface areas for TiO<sub>2</sub> is 159.6 m<sup>2</sup>/g. X-ray structure analysis Fig of the studied nanocomposite materials were recorded on the Rigaku Mini Flex 600s powder diffractometer. X-ray tube with copper anode (Cu-K $\alpha$  radiation, 30 kV and mA) was used to draw the diffraction specters at room temperature. At 2 $\theta$  = 20 $^{\circ}$ - 80 $^{\circ}$  with discrete growth mode these specters were obtained as  $\Delta 2\theta = 0.05^{\circ}$  and the exposure time was  $\tau = 5$  seconds.

The photochemical process lasted 1 hour using a very small amount of white powder and 0.05 gr of TiO<sub>2</sub> nanoparticles synthesized by the sol-gel method and N-containing substance. For the process 1 mgL<sup>-1</sup> of phenol solution was used. The process was monitored with a spectrophotometer "Varian Cary 50". After the photochemical decomposition of phenol, the reaction product was analyzed on an Agilent 6980N/5975 by the method GC-MSD. The goal was to determine the percentage of photochemical decomposition of phenol in TiO<sub>2</sub>+N system and 60% decomposition of phenol was defined.

**Key words:** Phenol; Degradation; X-ray diffraction; GC-MSD; nanoparticles.

### Introduction

The problem of pollution of aquatic ecosystems is one of the global environmental problems and it is important to have new more efficient cleaning methods [1]. Water-related problems, primarily related to global population growth and climate change require the introduction of new technologies to ensure the supply of drinking water and prevent global water pollution. In this regard, the use of nanotechnology and traditional technological processes opens up new ways to improve wastewater treatment technologies. This article discusses nanotechnological uses for the removal of toxic organic pollutants from wastewater [2].

Now cleaning methods using nanotechnological methods are widely utilized. There are many scientific articles on this topic in the literature. In addition, TiO<sub>2</sub> nanoparticles are currently used for various purposes [3].

According to the literature data free TiO<sub>2</sub> or its mixed systems are used in many photochemical reactions. These systems are mainly used to remove

organic toxic substances from wastewater. For example, nanotechnological methods are widely used to remove phenol and phenolic compounds from wastewater: the use of GO+Al<sub>2</sub>O<sub>3</sub> system for water purification is a very good method because 99.9% of phenol and its derivatives are removed from the wastewater [4]. Moreover decomposition of organic toxic substances from wastewater in the presence of TiO<sub>2</sub> nanoparticles is very common and we have done a lot of research on this [5]. Classical cleaning methods have always been included in chemistry. However, nowadays, nanotechnological purification methods are more promising and effective [6, 7]. Photochemical reactions have been studied using combined systems of TiO<sub>2</sub> with many metal oxides, nitrogen and activated carbon. Similar scientific works are found in the literature [8].

Many photochemical reactions have been studied using nitrogen fixing compounds. It is believed that photochemical reactions proceed faster with the formation of abundant oxygen particles as a result of the replacement of oxygen atoms of TiO<sub>2</sub> nanoparticles with nitrogen atoms with a similar

---

\*To whom all correspondence should be addressed.

electronic structure. At the same time, it is possible to expand the area of the photochemical process from UV to the visible area [9-13]. TiO<sub>2</sub>+N systems can be obtained in different ways. There is information about this in the literature [14-17]. Various nitrogen compounds can be used for this purpose [18]. However, it is not easy to find effective, simpler and less complex methods for the synthesis of TiO<sub>2</sub>+N; for this it is necessary to use systems that do not destroy the Ti-N bond. This requires systems that do not have a high temperature, since the chemical bond energy between Ti-O is higher than between Ti-N [19-22]. It is also known from the literature that TiO<sub>2</sub>+N systems could be obtained at high temperatures and for a long time [23-25]. From this point of view, we used nitrogen compounds together with TiO<sub>2</sub> nanoparticles [26].

The increase in the level of pollution of the world's oceans is currently one of the global environmental problems. The protection of the environment, especially the protection of aquatic ecosystems is currently a priority. New methods of wastewater treatment are needed. These problems can be solved by nanotechnological methods which are new and modern [27-29].

### Experimental

For the first time in a photochemical process the rutile form of TiO<sub>2</sub> was used, rather than anatase, which is the main factor that distinguishes our scientific work from other similar studies.

Recently nanotechnological approaches have become of chemical and environmental interest. Therefore we have carried out many photochemical studies with TiO<sub>2</sub> nanoparticles with a rutile phase and photochemical decomposition of phenol from water was achieved in high yield (99%) [30].

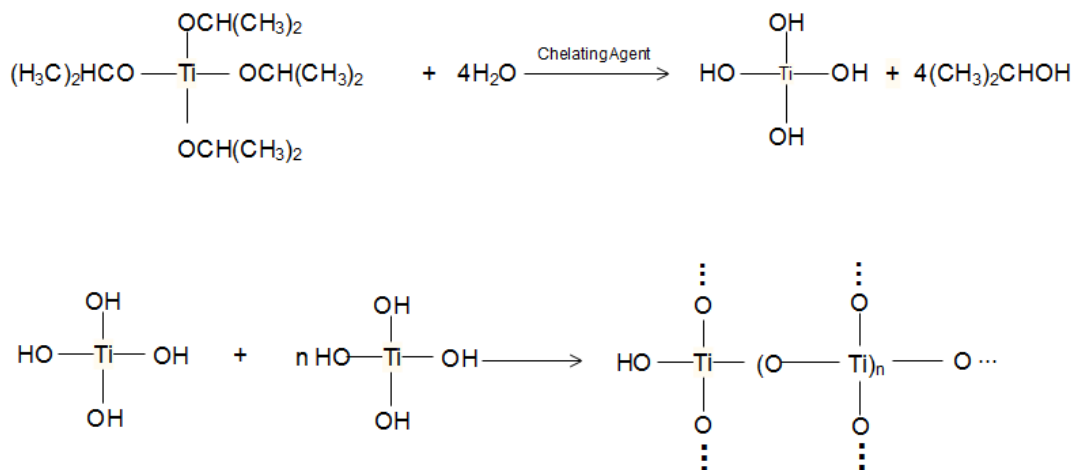
Since TiO<sub>2</sub> is a very good photochemical agent, the processes under consideration were studied in the presence of UV radiation. Later, in addition to TiO<sub>2</sub>, nitrogen-containing compounds were also used in the process and the transition of the process from the area of UV radiation to the visible area was observed. Many nitrogen compounds have been used for this purpose but the best results have been obtained with methyl-3-amicrotonate.

The process proceeded in the same way as in the TiO<sub>2</sub>+phenol system [30]. In the system TiO<sub>2</sub>+phenol the process took place only in the UV-radiation area but in the TiO<sub>2</sub>/N+ phenol system, the process took place in the UV-Visible area.

The reagents used in the photochemical process are:

20 ml of 1 mgL<sup>-1</sup> phenol solution, 0.05 grams of white powder of the TiO<sub>2</sub> nanoparticles of the rutile phase and 0.05 grams of N-organic matter in white case.

TiO<sub>2</sub> nanostructures are synthesized by the sol-gel method. This process proceeds through hydrolysis of titanium (IV) isopropoxide followed by condensation of formed Ti(OH)<sub>4</sub> (scheme).



Scheme-The hydrolysis of titanium (IV) isopropoxide.

The high rate of hydrolysis contributes to the formation of  $\text{Ti}(\text{OH})_4$  which interrupts the development of the chain Ti-O-Ti. The presence of a large number of Ti-OH groups and the low development of a three-dimensional polymer structure lead to a low particles packing.

As mentioned, methyl-3-amicrotonate was used as N substance in the photochemical process. Methyl 3-amicrotonate used for analysis was obtained in the laboratory using the following procedure:

50 ml of a solid  $\text{NH}_4\text{OH}$  solution and 10 ml of methylacetylacetone are added to a 100 ml volumetric flask. Stir for a long time with a magnetic stirrer. The mixing process should continue for 2-3 hours. The reaction mixture is decanted with chloroform and then washed with water, dried over  $\text{MgSO}_4$  and recrystallization is carried out as a result of which white crystals of methyl-3-amicrotonate are obtained. The formula of methyl-3-amicrotonate:  $\text{CH}_3\text{C}(\text{NH}_2)=\text{CHCOOCH}_3$

The photochemical process lasted 1 hour and the process was monitored on a "Varian Cary 50" spectrophotometer. In the end, the photochemical reaction mixture was analyzed by the GC-MSD method and the degradation of phenol was found to be 60%.

Quantitative analysis of phenols in aqueous samples was carried out on a gas chromatograph 6890N with a highly efficient mass selective detector Agilent 5975 manufactured by Agilent Technologies (USA). The instrument was equipped with a splitless injector. To separate the extract, a capillary column ZB-5 (Phenomenex)-5% diphenyl 95% dimethylpolysiloxane copolymer, 60 m long, with an inner diameter of 0.32 mm and a film thickness of 0.25  $\mu\text{m}$  was used. Helium was used as the carrier gas at a flow rate of 2.0 ml/min.

The degree of purity of helium is 99.999%. Ionizing source voltage is 70 eV, source temperature is 230°C, quadrupole temperature is 150°C and injector temperature is 270°C. The range of recorded masses is 30-500 daltons. The oven temperature rise was programmed from 40°C to 310°C. Shooting time was set to be 52 min. The SIM mode was used for the analysis. Compounds were identified using the WILEY and NIST mass spectra library as well as data from mass fragmentation processes. The introduction of samples was carried out using an automatic sampler.

In addition rutile phase of  $\text{TiO}_2$  nanoparticles was studied by TEM, XRD and SEM methods. The XRD and SEM analyzes were performed with the support of the "Laboratory of Nano-Research" of the Baku State University. The effect of pH on the process was also studied.

## Experimental

TEM, XRD, SEM were used to analyze the synthesized  $\text{TiO}_2$  nanoparticles. The prepared nano- $\text{TiO}_2$  was analyzed by TEM (Fig 1). As can be seen, the resulting nanoparticles grains are homogeneous.  $\text{TiO}_2$  nanoparticles have a spherical shape with a size of 10 to 30 nm; this agrees with the results calculated with the Scherrer method. The TEM analysis data correlate well with the results obtained by X-ray diffraction analysis.

By using the TEM method  $\text{TiO}_2$  nanoparticles were analysed. Transmission electron microscopy (TEM) analysis was used to determine the size of the nanoparticles to be around 10–30 nm while the Brunauer-Emmett-Teller (BET) specific surface area of the rutile nanoparticle was 159.6  $\text{m}^2/\text{g}$ .

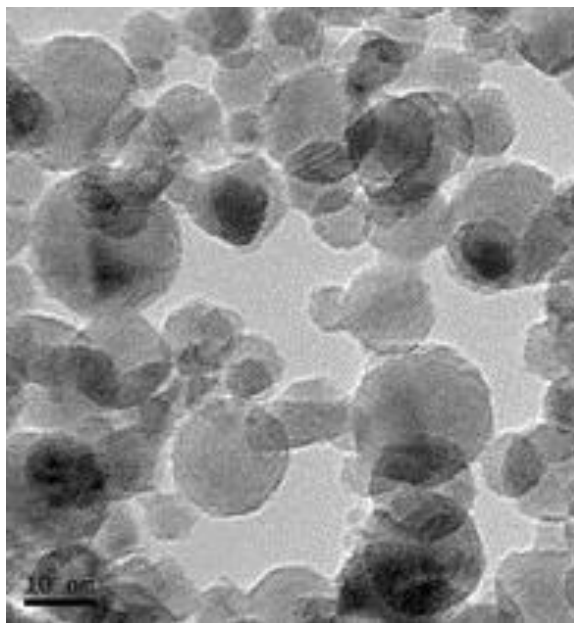


Fig. 1: TEM analysis of the rutile phase  $\text{TiO}_2$  nanoparticles.

Fig 2 shows the XRD patterns of the synthesized  $\text{TiO}_2$  nanoparticles. All the XRD peaks were well defined and corresponded to  $\text{TiO}_2$  at rutile phase [31].

Fig 2 shows the XRD patterns of the synthesized TiO<sub>2</sub> nanoparticles. It can be seen that all the XRD peaks are well-defined and correspond to rutile phase TiO<sub>2</sub>. From the line broadening of the (101) diffraction peak by Scherrer's method, the average crystal size of TiO<sub>2</sub> is about 10.3. The specific surface area of TiO<sub>2</sub> is about 159.6 m<sup>2</sup>/g. In the pattern, all lines can be indexed using the ICDD (PDF-2/ Release 2011 RDB) DB card number 00-001-1292. The pattern of TiO<sub>2</sub> nanoparticles has characteristic peaks

at 27.90° (110), 36.01° (101), 41.58 (111), 54.71° (211).

Scanning electron microscopy (SEM) analyzes provide high resolution images of single nanoparticles well below 10 nm in size. With the SEM method TiO<sub>2</sub> nanoparticles were analysed (Fig 3). The sizes of rutile phase TiO<sub>2</sub> nano-particles were found to be between 10 and 30 nm.

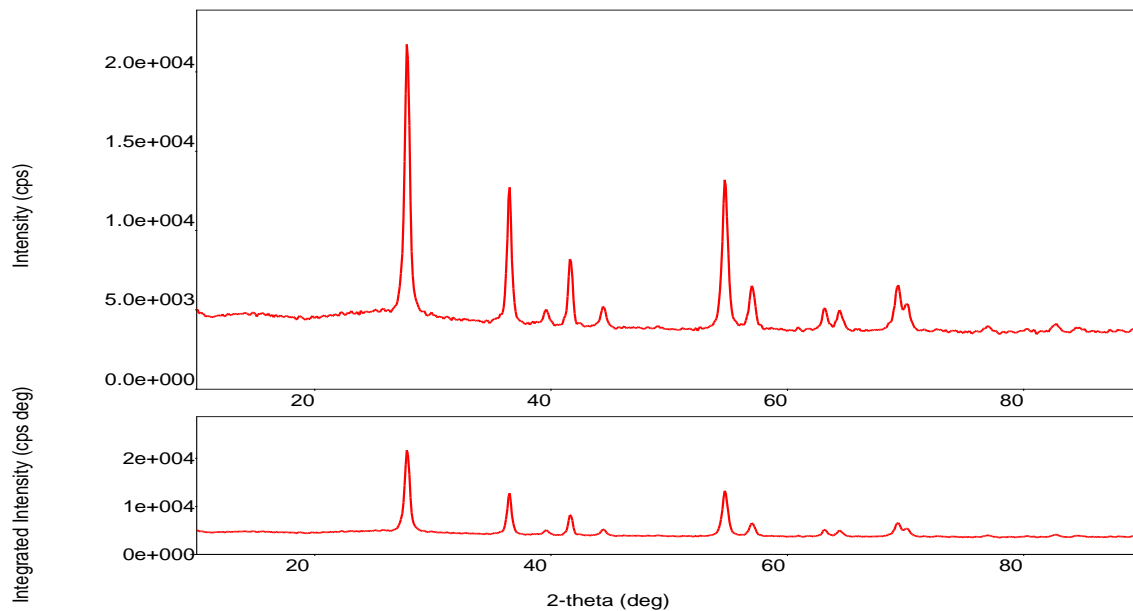


Fig. 2: XRD patterns of the rutile phase TiO<sub>2</sub> nanoparticles.

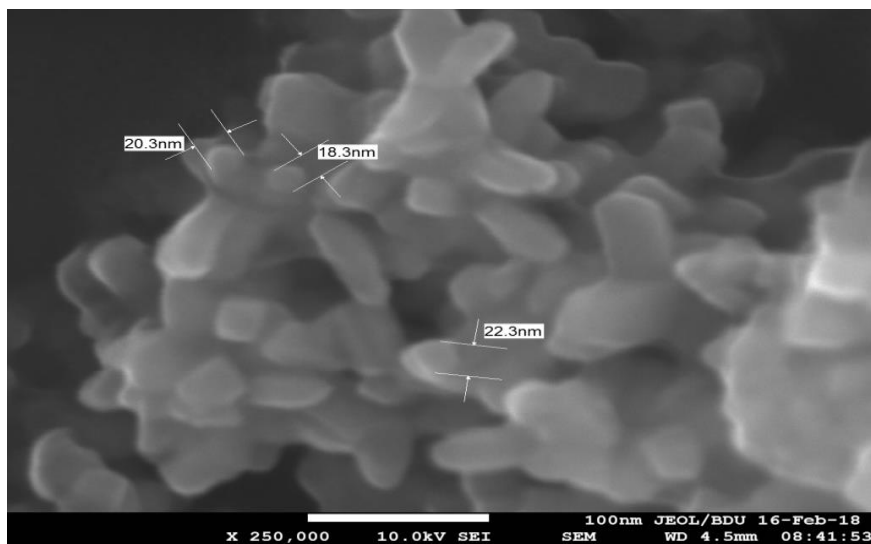


Fig. 3: SEM analysis of the rutile phase TiO<sub>2</sub> nanoparticles.

Also the light irradiation of  $\text{TiO}_2$  nanoparticles was studied. The highest peaks were recorded in the range of 300–350 nm wavelengths upon excitation of  $\text{TiO}_2$  nanoparticles with UV radiation [31].

## Results and Discussion

The curve in Fig 4 was plotted on a spectrophotometer prior to the photochemical process. It should be noted that since no dissociation of phenol occurred in the process characteristic signals for 270 nm were observed. As can be seen in Fig. 4, phenol-similar curves have been taken at 200–300 nm. It is also known from the literature that the curve obtained at 270 nm wavelengths corresponds to that of phenol [30].

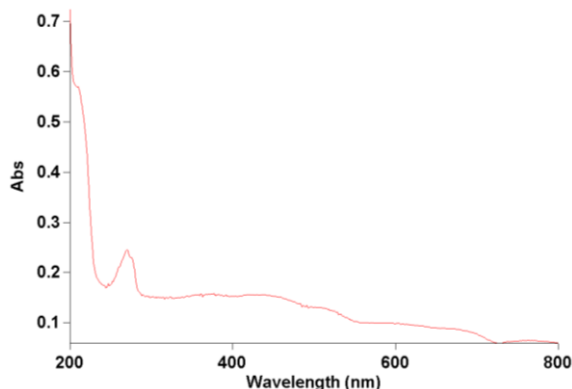


Fig. 4: Comparison of the curve obtained before the photolysis process.

In Fig 5 it is given the comparison of the curves obtained after photolysis process. It is seen from the Fig 5 that the curves which are characteristic for phenol (270 nm) is reducing gradually so that it is the dissociation of phenol in the photochemical process. Curve 1 is the obtained in the process before photolysis. As can be seen, a phenol-corresponding curve was observed at 270 nm as the photolysis process did not proceed. However, for phenol after curves 2, 3, 4, 5, 6, these signals were not obtained or were identified very faintly.

This indicates that the photolysis process is underway. The photolysis process was monitored with a “Varian Cary 50” spectrophotometer.

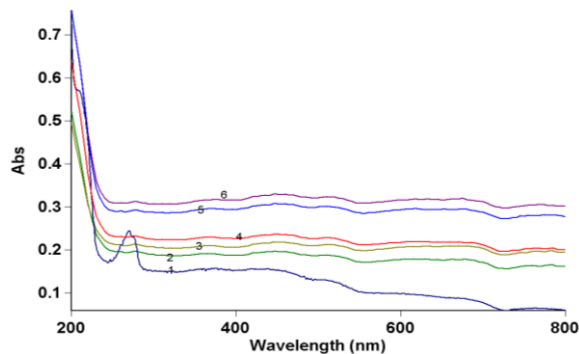


Fig. 5: UV irradiation after the photolysis process in the system phenol+methyl-3-aminocrotonate+ $\text{TiO}_2$ .

Characters of each curves are given below:  
Curve 1- $\text{TiO}_2/\text{N}$ +phenol before photolysis;

The comparison of UV radiation curves obtained from the photolysis process:

Curve 2-in the 60th minute of photolysis; curve 3-in the 55th minute of photolysis; curve 4-in the 50th minute of photolysis; curve 5-in the 45th minute of photolysis; curve 6-in the 40th minute of photolysis.

The influence of the pH of the medium on the course of the reaction was also studied. It was found that at pH=4 the photochemical reaction is better and the decomposition of phenol is higher (Fig 6).

Fig 6 shows that the photochemical dissociation of phenol proceeded at the maximum pH = 4. On the contrary at pH=8 the destruction of phenol occurred very slightly. This suggests that the degradation of phenol in an acidic environment is better than in an alkaline one.

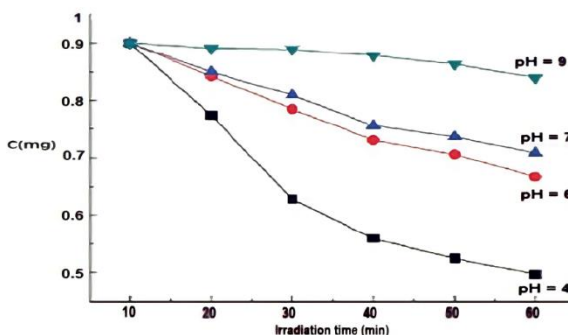


Fig. 6: Dependence of the photochemical decomposition of phenol on pH.

On the contrary after the UV radiation field certain curves were obtained that fell into the visible

area of this field. Hence the process took place in the UV-Visible area (Fig 7).

Fig 7 below shows the doping of nitrogen atoms on a molecule of TiO<sub>2</sub> nanoparticles: As can be seen from Fig7 the photochemical dissociation of phenol in the presence of TiO<sub>2</sub> nanoparticles occurred in the UV area i.e. in the area up to 400 nm. However in the presence of organic matter N and TiO<sub>2</sub> (TiO<sub>2</sub>/N) the process propagated from the UV area to the visible area (from 400 nm to 600 nm).

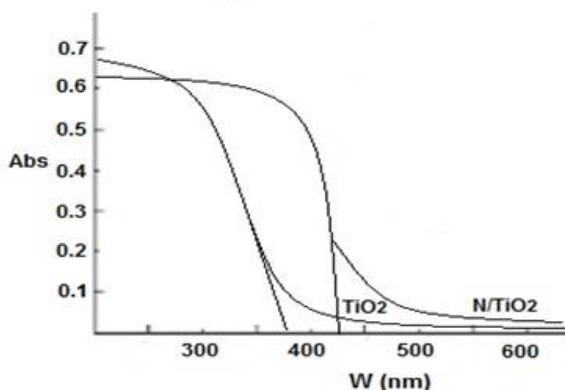
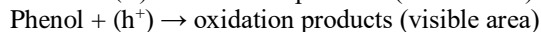
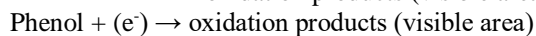
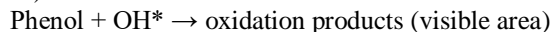
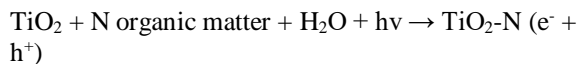


Fig. 7: N-doped TiO<sub>2</sub> spectroscopy of the rutile phase nanoparticles.

It is assumed that the mechanism of TiO<sub>2</sub> with N proceeds as follows. Nitrogen replaces oxygen in the TiO<sub>2</sub> molecule.



After the photochemical process, the sample was analyzed with the GC-MSD method. Quantitative analysis of the samples was carried out on an Agilent 5975 GC/MS high performance mass selector detector equipped with a 6890N gas chromatograph. The sample was retrieved. The solvents used were methylene chloride and dichloromethane for extraction. The amount of phenol dropped from 1 mg to 0.4 mg. The following is the chromatographic curves of the sample after the photolysis process (Fig 8).

After the quantitative analysis, 40% of phenol remained in the solution. In the presence of methyl 3-aminocrotonate phenol degradation was 60%.

In the end, we can say that in the presence of an N-containing compound the process took place in the UV-Visible area which increased the practicality of the photocatalytic process.

The article is devoted to the neutralization of toxic organic substances in the aquatic system. In the future these studies will be continued using various TiO<sub>2</sub> and another systems.

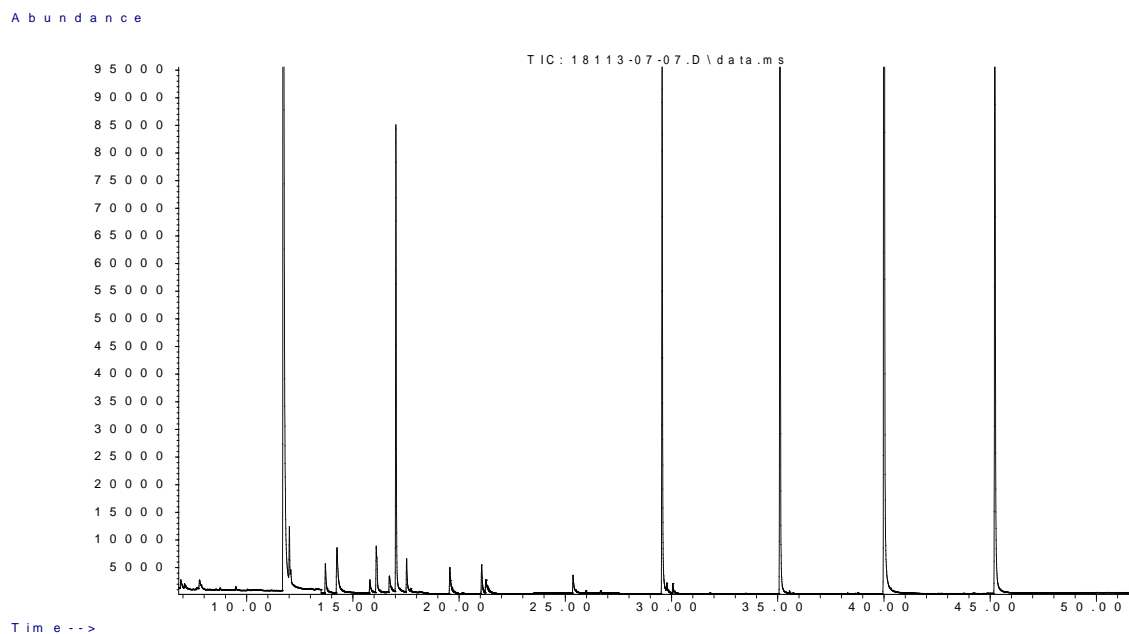


Fig. 8: General view of chromatogram of 1 mgL<sup>-1</sup> phenol solution after photochemical degradation.

## Conclusion

Recently, the purification of aquatic ecosystems using nanotechnological methods is one of the most important issues from an environmental point of view. To do this environmentally friendly TiO<sub>2</sub> nanoparticles were used. TiO<sub>2</sub> nanoparticles have excellent catalytic properties in photochemical processes as they are also environmentally friendly. The rutile modification of TiO<sub>2</sub> was used for the first time in photochemical process. Methyl 3-amicronate was used as a nitrogen-retaining agent in the process. The purpose of using a nitrogenous substance was to carry out a photochemical reaction in the visible area in the presence of TiO<sub>2</sub> nanoparticles in the UV area of radiation. This increases the practical significance of the process. Sizes of the used TiO<sub>2</sub> nanoparticles were between 10 and 30 nm. Decomposition of 1 mgL<sup>-1</sup> phenol was carried out for 1 hour. The photochemical degradation of phenol in the TiO<sub>2</sub>/N system was 60%. In the process, the influence of the pH of the medium on the course of the reaction was determined. The process was monitored with a “Varian Cary 50” spectrophotometer. In addition, TEM, SEM, X-ray diffraction analysis of nanoparticles was carried out. Quantitative analyzes were determined by the GC-MSD Agilent 6980N/5975.

## Conflicts of interests

The authors declare that no conflicts of interests.

## Acknowledgment

The analysis was performed with the support of the “Nano Research Laboratory” of Baku State University. We are very thankful to head of laboratory for the opportunity to work there.

## REFERENCES

1. S. Khan, Mu. Naushad, Muthusamy Govarthan, *et al*, Emerging contaminants of high concern for the environment: Current trends and future research, *J. Env. Res*, **207**, 112609 (2022).
2. Shamshad Khan, Mu. Naushad, Adel Al-Gheethi, Jibran Iqbal, Engineered nanoparticles for removal of pollutants from wastewater: Current status and future prospects of nanotechnology for remediation strategies, *J. Env. Che. Eng.*, **9**, 106160 (2021).
3. Niloufar Torkian, Abbas Bahrami, Afrouzossadat Hosseini, *et al*, Synthesis and characterization of Ag-ion-exchanged zeolite/TiO<sub>2</sub> nanocomposites for antibacterial applications and photocatalytic degradation of antibiotics, *J. Env. Res*, **207**, 112157 (2022).
4. H. Xuebing; Yu, Yun, R. Shuang, L. Na; W. Yongqing; Z., Jianer, Highly efficient removal of phenol from aqueous solutions using graphene oxide/Al<sub>2</sub>O<sub>3</sub> composite membrane, *J. Por. Mat.*, **25**, 719 (2018).
5. C. Santhosh, V. Velmurugan, G. Jacob, S. K. Jeong, A. N. Grace, A. Bhatnagar, Role of nanomaterials in water treatment applications, *J. Chem. Eng.*, 1116 (2016).
6. F. Wang, Novel high performance magnetic activated carbon for phenol removal: equilibrium, kinetics and thermodynamics, *J. Por. Mat.*, **24**, 1 (2017).
7. Y. Li, W. Cao, F. Ran and X. Zhang, Photocatalytic degradation of methylene blue aqueous solution under visible light irradiation by using N-doped titanium dioxide, *Eng. Mat.*, **338**, 1972 (2007).
8. Amir Sada Khan, Taleb H. Ibrahim, Mustafa I. Khamis, *et al*, Preparation of sustainable activated carbon-alginate beads impregnated with ionic liquid for phenol decontamination, *J. Clean. Prod.*, **321**, 12889 (2021).
9. J. Xu, F. Wang, W. Liu and W. Cao, Nanocrystalline N-Doped TiO<sub>2</sub> Powders: Mild Hydrothermal Synthesis and Photocatalytic Degradation of Phenol under Visible Light Irradiation, *Pub. Corp.*, 1 (2013).
10. X. Qiu and C. Burda, Chemically synthesized nitrogen-doped metal oxide nanoparticles, *Chem. Phys.*, **339**, 1 (2007).
11. D. Wu, M. Long, W. Cai, C. Chen and Y. Wu, Low temperature hydrothermal synthesis of N-doped TiO<sub>2</sub> photocatalyst with high visible-light activity, *J. of All. and Comp.*, **502**, 289 (2010).
12. N. Bao, J. J. Niu, Y. Li, G. L. Wu and X. H. Yu, Low-temperature hydrothermal synthesis of N-doped TiO<sub>2</sub> from small-molecule amine systems and their photocatalytic activity, *Env. Tech.*, **1** (2012).
13. R. Asahi, T. Morikawa, T. Ohwaki, K. Aoki and Y. Taga, Visible-light photocatalysis in nitrogen-doped titanium oxides, *Scien.*, **293**, 269 (2001).
14. S. Z. Hu, F. Y. Li and Z. P. Fan, The influence of preparation method, nitrogen source and post-treatment on the photocatalytic activity and stability of N-doped TiO<sub>2</sub> nanopowder, *J. Haz. Mat.*, **196**, 248 (2011).
15. B. Baruwati and R. S. Varma, Synthesis of N-doped nano TiO<sub>2</sub> using guanidine nitrate: an excellent visible light photocatalyst, *J. Nanosci. and Nanotech.*, **11**, 2036 (2011).
16. S. Livraghi, A. M. Czoska, M. C. Paganini and E. Giamello, Preparation and spectroscopic

- characterization of visible light sensitized N doped TiO<sub>2</sub>, *J. Solid State Chem.*, **182**, 160 (2009).
17. M. Darienzo, R. Scotti, L. Wahba et al., Hydrothermal N-doped TiO<sub>2</sub>: explaining photocatalytic properties by electronic and magnetic identification of N active sites, *J. Appl. Catal.* **93**, 149 (2009).
  18. H. Diker, C. Varlikli, K. Mizrak, and A. Dana, Characterizations and photocatalytic activity comparisons of N-doped n-TiO<sub>2</sub> depending on synthetic conditions and structural differences of amine sources, *Energy*, **36**, 1243 (2011).
  19. M. H. Chan and F. H. Lu, Characterization of N-doped TiO<sub>2</sub> films prepared by reactive sputtering using air, *Thin Solid Films*, **518**, 1369 (2009).
  20. W. Guo, Y. Shen, G. Boschloo, A. Hagfeldt and T. Ma, Influence of nitrogen dopants on N-doped TiO<sub>2</sub> electrodes and their applications in dye-sensitized solar cells”, *Electro. Acta*, **56**, 4611 (2011).
  21. Y. Wang, C. Feng, M. Zhang, J. Yang and Z. Zhang, Visible light active N-doped TiO<sub>2</sub> prepared from different precursors: origin of the visible light absorption and photoactivity, *J. App. Cat.*, **104**, 268 (2011).
  22. D. Huang, S. Liao, S. Quan, et al. Synthesis and characterization of visible light responsive N-TiO<sub>2</sub> mixed crystal by a modified hydrothermal process, *J. Non-Crys. Sol.*, **354**, 3965 (2008).
  23. A. O. Ibadon, P. Fitzpatrick, Heterogeneous Photocatalysis: Recent Advances and Applications, *Catalysts*, **3**, 1 (2013).
  24. Al-Rasheed R. A. Jeddah., *Water Treatment by Heterogeneous Photocatalysis: Saline Water Desalination* Research Institute, Saudi Arabia, 14 (2005).
  25. X. Qiu and C. Burda, Chemically synthesized nitrogen-doped metal oxide nanoparticles, *J. Chem. Phys.*, **339**, 1 (2007).
  26. Y. Li, W. Cao, F. Ran and X. Zhang, Photocatalytic degradation of methylene blue aqueous solution under visible light irradiation by using N-doped titanium dioxide, *Key Engin. Mat.*, **338**, 1972 (2007).
  27. H. Q. Wang, Z. B. Wu and Y. Liu, A simple two-step template approach for preparing carbon-doped mesoporous TiO<sub>2</sub> hollow microspheres, *J. Phys. Chem.*, **113**, 13317 (2009).
  28. K. Huang, L. Chen, M. Liao and J. Xiong, The photocatalytic inactivation effect of Fe-doped TiO<sub>2</sub> nanocomposites on Leukemic HL60 cells-based photodynamic therapy, *J. Photoenergy*, **8** (2012).
  29. P. Chowdhury, J. Moreira, H. Goma and A. K. Ray, Visible-solar-light-driven photocatalytic degradation of phenol with dye-sensitized TiO<sub>2</sub>: parametric and kinetic study, *Indus. & Eng. Chem. Res.*, **51**, 4523 (2012).
  30. E. M. Gadirova, Photochemical degradation of phenol in the presence of titanium dioxide nanoparticles, *J. App. Chem. and Biotech.*, **9**, 176 (2019).
  31. E. M. Gadirova, S. R. Hajiyeva and A. R. Sujayev, Investigation of photocatalytic properties of TiO<sub>2</sub> nanoparticles belonging to rutile phase, *J. Mol. Str.* **1227**, 129534 (2021).